Experimental performance of polymeric air-solution contactors for liquid desiccant systems

Juan Prieto*, Jordi Ortiga, Alberto Coronas

*CREVER, Mechanical Engineering Department, Universitat Rovira i Virgili. Avda Països Catalans 26, 43007, Tarragona (Spain). +34 977 25 78 91, corresponding author: juan.prieto@urv.cat,

Abstract

This paper evaluates the experimental performance of two falling-film absorbers with horizontal tubes of a liquid desiccant system. Both absorbers are made of polypropylene in order to avoid corrosion when the LiCl-H_2O solution is in contact with them. To improve their wettability, and hence the heat and mass transfer, the tubes from one of the absorbers are subject to a plasma surface treatment. According to the experimental results, the inlet liquid desiccant temperature and air velocity are the variables that most affect the absorber performance. Therefore, these two variables can be used to control the supply humidity ratio and air cooling rate in a liquid desiccant system. Furthermore, in comparison with the absorber with untreated tubes, the absorber with treated tubes performed better in terms of the overall heat transfer coefficient (up to 54 %), the absorber heat duty (about 17 %), the air cooling rate (up to 29 %) and the dehumidification rate (20 %).

Keywords*: Liquid desiccants, Experimental Performance, Absorber, Falling-film, Polypropylene, Plasma Surface Treatment.*

Nomenclature

A	Contact surface (m^2)	W	Humidity ratio (kg_w/kg_{da})
c_p	Specific heat capacity (kJ/kg·K)	X	Lithium Chloride mass fraction (-)
d	Tube diameter (m)	μ	Dynamic viscosity (N-s/m^2)
F	Correction factor for ΔT_{LM} method (-)	Γ	Solution mass flow rate per tube length (kg/m·s)
g	Gravity acceleration (9.81 m/s^2)	$\Delta\Omega$	Dehumidification (kg_w/m^2·s)
h	Specific enthalpy (kJ/kg)		
H	Humidity ratio (%)		
L	Length (m)	*Subscripts*	
m	Mass flow rate (kg/s)	a	Air flow
Q	Cooling/heating rate (kW)	in	Inlet
Re_s	Reynolds number of the solution flow ($2\,\Gamma_s/\,\mu_s$) (-)	lat	Latent
		out	Outlet
T	Temperature (K)	s	Solution flow
U	Overall heat transfer coefficient (kW/m^2·K)	sen	Sensible
v	Volumetric flow rate (l/h)	t	Tube
V	Velocity (m/s)	w	Water flow

1. Introduction

In applications in which dehumidification is important, liquid desiccant systems are a good alternative to vapor compression systems ([1], [2]) because they achieve very low levels of humidity and can be driven by low-grade heat sources. They also operate without greenhouse gases [3] and can be used in combination with vapor compression systems to control humidity and temperature separately and more efficiently [4–6].

The main parts of a liquid desiccant system (Figure 1) are the two air-solution contactors: the absorber and the desorber [7]. In the absorber, moist air is dehumidified by direct contact with the liquid desiccant in an exothermic process and, therefore, cooling is required to remove the heat produced during the dehumidification process. In the desorber, the water absorbed is released by direct contact with moist air in an endothermic process, so heating is required to regenerate the solution through this component. A solution-solution heat exchanger is often added to improve the performance of the system. Sometimes, it is also recommended to include liquid desiccant storage as a buffer.

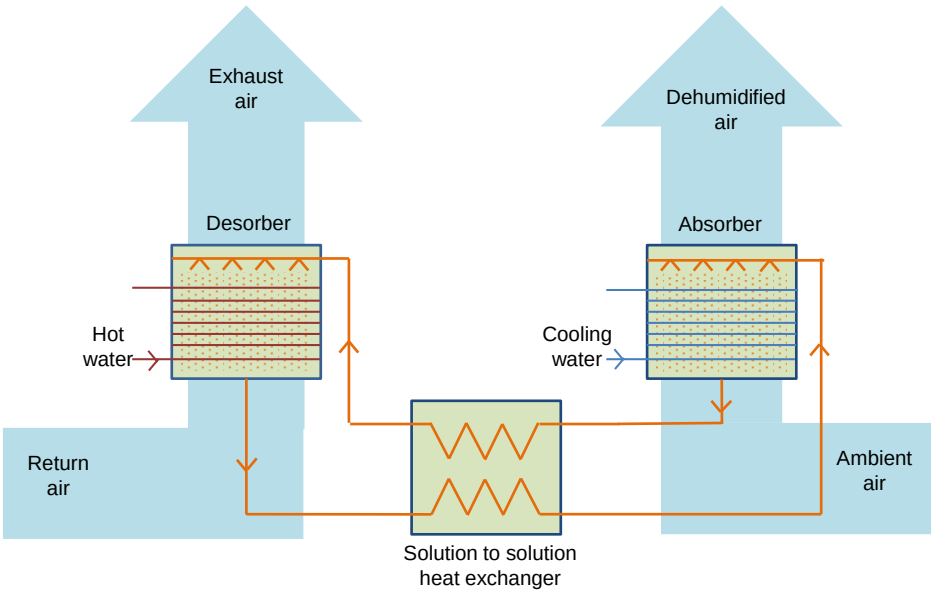

Figure 1. Schematic figure of a liquid desiccant system [7]

Most of the absorbers and desorbers in the liquid desiccant systems of commercial and scientific applications ([8–13]) are made of packed-bed material working as an adiabatic air-solution contactor, because of its low price and high contact surface area. However, non-adiabatic air-solution contactors are now being studied ([14–18]) because they require lower liquid desiccant flow rates to achieve the same dehumidification. This increases the change in concentration of the liquid desiccant material throughout the air-solution contactors and, therefore, increases the chemical storage and COP of the system. Moreover, carry-over, one of the main problems of liquid desiccant systems, is reduced [12], [19].

The most common working fluid mixture used in liquid desiccant systems is LiCl-H_2O because of its low vapour pressure. However, this solution corrodes most metals except for titanium and tantalum, which are very expensive. For this reason, plastic materials could be a good cost-competitive alternative for these applications despite their poorer thermal conductivity and wettability. Tube wetting is a key issue to be solved in falling-film plastic tubes because affects to both the wetted area and the film thickness. Therefore, the better the tube wetting the higher both the overall heat transfer coefficient and the water absorption.

Furthermore, this desiccant material has high surface tension, which makes tube wetting even more difficult. Gommed et al. [20] made a comparison of three absorbers: an adiabatic packed-bed absorber, a falling-film on horizontal tubes absorber made of titanium and a falling-film on horizontal tubes absorber made of high density polyethylene. Overall heat transfer coefficient achieved by the titanium absorber was 332 $W/m^2 \cdot K$ and by the high density polyethylene absorber 147 $W/m^2 \cdot K$. From this comparison, it was concluded that the

poorer dehumidification and heat transfer in the plastic air-solution contactor were mainly due to its lower wettability.

The main objective of this study is to experimentally evaluate the enhancement of the absorber performance of a falling-film on horizontal tubes absorber made of polypropylene with a plasma surface treatment on the outside of the tubes, which consists of plasma nano-layer depositions of acrylic acid [21]. Plasma surface treatment increases the tube wetting. This performance is compared to the performance of an absorber with the same specifications but with standard polypropylene tubes. Results are also given for how different conditions of air, water and LiCl-H_2O solution affect the absorber performance.

2. Material and methodology

2.1. Description of the experimental test facilities

A test bench was built in order to study the dehumidification process of two absorbers with horizontal polypropylene tubes and LiCl-H_2O solution. Figure 3 shows a schematic of the test bench which can be divided into three different subsystems:

- The liquid desiccant circuit (green lines) which contains two solution reservoirs so that the test bench can be operated discontinuously in order to supply a homogeneous liquid desiccant mass fraction to the absorber, a pump with a frequency driver, valves and sensors (temperature and flow rate).
- The water subsystem (red lines) which consists of a water chiller, a water boiler, an electric water heater, two pumps, valves and sensors (temperature and flow rate).
- The air subsystem which consists of a fan with a frequency driver, a humidifier, a heating coil and sensors (temperature, relative humidity and air velocity).

All the components in contact with the LiCl-H_2O solution are made of non-corrosive materials.

Table 1contains the specifications of the tested absorbers. Both have the same dimensions, number of tubes and tube arrangement. This makes a direct comparison between them possible. Figure 2 shows a drawing and a picture of one of the air-solution contactors when it was placed inside the polycarbonate tower (see Figure 3). The absorbers only have a pass cooling system.

Table 1. Specifications of the tested air-solution contactors

Number of columns	4
Total number of tubes	78
Tube length (mm)	325
Outlet tube diameter (mm)	6.5
Inlet tube diameter (mm)	5.1
Tube arrangement	Staggered
Column distance (mm)	10.5
Row distance (mm)	14.4
Thermal conductivity of tubes (W/m·°C)	0.21

Figure 2. Falling-film air-solution contactor

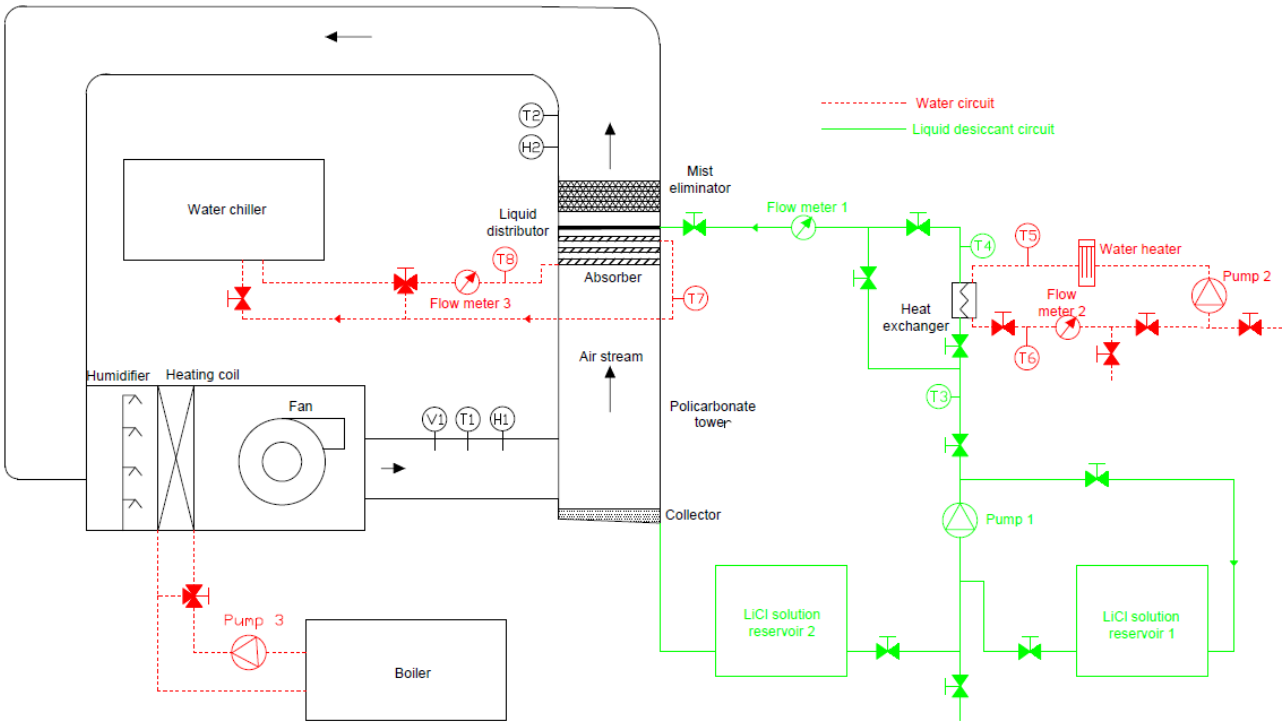

Figure 3. Schematic of the test bench for the absorber study

The parameters measured, the measurement devices, their accuracies and operational ranges are listed in Table 2. These values are required for the uncertainty calculations. All the parameters were scanned and recorded using an Agilent 34970A data acquisition system. The only exception was the density measurements, which were collected by an Anton-Paar DMA 35 portable density meter.

Table 2. Specifications of the measuring devices

Parameter	Device	Accuracy	Operational Range
Water and desiccant temperature sensors	Calibrated Pt100	0.01 ºC	0-100 ºC
Water flow rate	Water flow meter	0.4 %	0-400 l/min
Desiccant flow rate	Electromagnetic flow meter	0.3 %	0-150 l/min
Air temperature	Air temperature sensor	0.2 ºC	-20 - +80 ºC
Air relative humidity	Air relative humidity sensor	2 %	0-100 %
Air velocity	Air velocity sensor	0.3 m/s+ 3 %	0-10 m/s
Liquid desiccant density	Density meter	0-0.001 cm^3	0-3 g/cm^3

2.2. Methodology

Figure 4 shows a schematic of the absorber that includes the inlets and outlets of the streams and the measured variables. Both the moist and the liquid desiccant, which are in direct contact outside the horizontal tubes, are in counter-current flow. Cooling water is required inside the tubes to cool the solution at the same time as the water is being absorbed. In this way, the dehumidification process is more homogenous using an internally-cooled absorber than using an adiabatic absorber. This is an advantage over the adiabatic absorbers, in which the liquid desiccant is heated throughout the absorber due to the absorption process, so the dehumidification process is less effective. The overall heat transfer coefficient, the absorber heat duty, the air cooling rate, and the dehumidification rate were the parameters chosen to assess the absorber's performance.

The following parameters were measured:

- Air velocity, V_a (m/s)
- Inlet air temperature, $T_{a,in}$ (°C)
- Inlet air relative humidity, $H_{a,in}$ (%)
- Outlet air temperature, $T_{a,out}$ (°C)
- Outlet air relative humidity $H_{a,out}$ (%)
- Inlet water temperature, $T_{w,in}$(°C)
- Outlet water temperature, $T_{w,out}$ (°C)
- Volumetric water flow rate, $v_{w,in}$ (l/h)
- Inlet solution temperature, $T_{s,in}$ (°C)
- Outlet solution temperature, $T_{s,out}$ (°C)
- Volumetric solution flow rate, $v_{s,in}$ (l/h)
- Inlet solution density, $\rho_{s,in}$ (kg/m^3)
- Outlet solution density, $\rho_{s,out}$ (kg/m^3)

The thermo-physical properties for moist air are taken from Hyland and Wexler [22] and the thermodynamic properties for water from Haar et al. [23]. The specific enthalpy and density of the LiCl-H_2O solution were calculated using equations from Pátek and Klomfar [24]. However, viscosity was taken from the correlations in Conde [25].

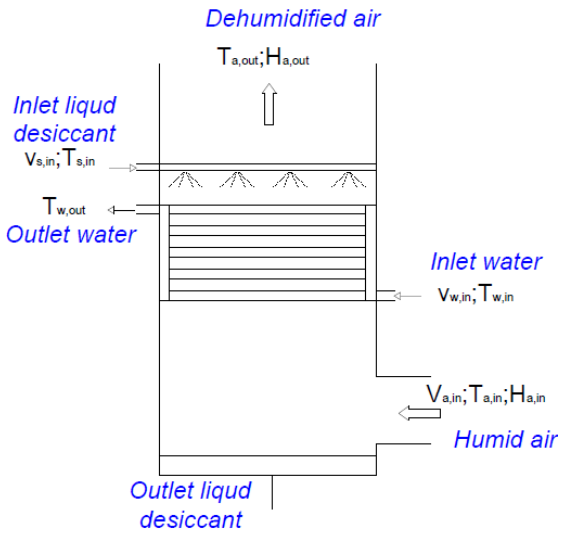

Figure 4. Schematic with the absorber inlets and outlets and the measured variables

The water absorbed on the outer contact surface of the tubes can be obtained from air stream measurements by using the following equation:

$$\Delta\Omega = \frac{\dot{m}_{a,in}}{A} \cdot (W_{a,in} - W_{a,out}) \quad (1)$$

where A is the contact surface between the solution film and the tubes, which is considered equal to the external surface of the tubes. Therefore:

$$A = \pi \cdot d_o \cdot L_t \cdot n_t \quad (2)$$

The absorber heat duty can be calculated by the sensible heat equation in the water stream as it is presented in the following equation:

$$\dot{Q}_w = \dot{m}_{w,in} \cdot (c_{p,w,out} \cdot T_{w,out} - c_{p,w,in} \cdot T_{w,in}) \quad (3)$$

The overall heat transfer coefficient can be calculated as:

$$U = \frac{\dot{Q}_w}{A \cdot \Delta T_{LM}} \quad (4)$$

where ΔT_{LM} is the logarithmic mean temperature difference, which in this case is calculated as:

$$\Delta T_{LM} = F \cdot \Delta T_{LM,ccf} \quad (5)$$

$\Delta T_{LM,ccf}$ is the logarithmic mean temperature difference between the water stream and the LiCl-H_2O solution stream at counter-current flow. That is:

$$\Delta T_{LM,ccf} = \frac{(T_{s,in} - T_{w,out}) - (T_{s,out} - T_{w,in})}{\ln \frac{(T_{s,in} - T_{w,out})}{(T_{s,out} - T_{w,in})}} \quad (6)$$

F is the correction-factor plot for the single-pass cross-flow exchanger – one fluid mixed, the other unmixed – which is obtained according to the correlation presented by Bowman et al. [26].

The air cooling rate is calculated as the addition of sensible cooling and latent cooling since both the temperature and humidity of moist air change through the absorber. This means:

$$\dot{Q}_a = \dot{Q}_{sen} + \dot{Q}_{lat} \quad (7)$$

where sensible cooling is related to change in the moist air temperature, so:

$$\dot{Q}_{sen} = \dot{m}_{a,in} \cdot (c_{p,a,in} \cdot T_{a,in} - c_{p,a,out} \cdot T_{a,out}) \quad (8)$$

and latent cooling is related to change in the moist air humidity ratio, so:

$$\dot{Q}_{lat} = \dot{m}_{a,in} \cdot h_{c,w} \cdot (W_{a,in} - W_{a,out}) \quad (9)$$

The energy balance of the absorber is an extra equation used as a validating equation. It is calculated by the following equation:

$$\dot{Q}_a - \dot{Q}_w + \dot{Q}_s = 0 \quad (10)$$

where $\dot{Q}_s$ is the heating/cooling rate of the liquid desiccant, which can be calculated as:

$$\dot{Q}_s(kW) = \dot{m}_{s,in} \cdot h_{s,in} - \dot{m}_{s,out} \cdot h_{s,out} \quad (11)$$

where the outlet liquid desiccant mass flow rate and mass fraction are obtained from water and liquid desiccant mass balance equations:

$$\dot{m}_{a,in} \cdot (W_{a,in} - W_{a,out}) = \dot{m}_{s,out} \cdot (1 - X_{s,out}) - \dot{m}_{s,in} \cdot (1 - X_{s,in}) \quad (12)$$

$$\dot{m}_{s,out} \cdot X_{s,out} = \dot{m}_{s,in} \cdot X_{s,in} \quad (13)$$

where inlet and outlet liquid desiccant mass fractions are obtained from density and temperature measurements. The air-solution contactors were tested in absorber working conditions.

Table 3 shows the experimental conditions of both air-solution contactors. It should be pointed out that most of the conditions were modified independently and the other variables were kept constant in order to determine their effect on the absorber performance. However, inlet air relative humidity and the LiCl mass fraction were not changed independently because of restrictions of the test bench.

Table 3. Experimental conditions of treated and standard polypropylene air-solution contactors

Experimental conditions	Treated absorber	Standard absorber
Air velocity (m/s)	1.12-2.09	0.99-2.10
Solution flow rate (l/h)	122.5-343.8	113.3-314.7
Water flow rate (l/h)	321.7-423.5	220.7-325.7
Inlet water temperature (°C)	8.7-17.9	8.7-15.3
Inlet solution temperature (°C)	17.9-25.0	17.0-23.8
Inlet air temperature (°C)	29.5-33.6	27.0-32.6
Inlet air relative humidity (%)	33.2-46.6	35.5-48.5
LiCl mass concentration (%)	35.3-35.7	35.7-35.9

3. Results and discussion

The absorber with standard tubes was tested in 24 experimental conditions, whereas the absorber with treated tubes was tested in 26. The appendix contains the experimental measurements obtained during these tests. As is mentioned above, the overall heat transfer coefficient, absorber heat duty, air cooling rate, and dehumidification rate were the parameters chosen for assessing the absorber performance. Section 3.1 describes the absorber performance under different working conditions, whereas Section 3.2 compares the two absorbers. A detailed error analysis was made as described in [27]. Table 4 includes the maximum uncertainties of the absorber performance parameters with a 95 % confidence interval.

Table 4. Maximum uncertainty of the absorber performance parameters.

Absorber	Maximum uncertainty of heat duty (kW/m^2)	Maximum uncertainty of air cooling rate (kW/m^2)	Maximum uncertainty of overall heat transfer coefficient ($kW/°C \cdot m^2$)	Maximum uncertainty of dehumidification rate ($kg_w/s \cdot m^2$)
Standard tubes	± 0.15	± 0.11	± 0.012	$\pm 3.7 \cdot 10^{-5}$
Treated tubes	± 0.17	± 0.13	± 0.015	$\pm 3.1 \cdot 10^{-5}$

3.1. Absorber performance

The overall heat transfer coefficient (Figure 5) depends not only on the water flow rate but also on the air velocity and the Reynolds number of the liquid desiccant flow. The higher the air velocity, the higher the

absorber heat duty is. Therefore, at this range of air velocities, heat transfer is enhanced due to the beneficial effect of the air velocity on the solution-tube heat transfer coefficient that was also experienced by Ambruster and Mitrovic [28]. However, according to our previous studies [7], air velocities higher than 2.5 m/s lead to liquid desiccant carry-over and the formation of dry patches on tubes, which deteriorates the heat transfer. On the other hand, the solution mass flow rate has an effect on the overall heat transfer coefficient at Reynolds numbers higher than 18 on the standard tubes but at lower values in the absorber with treated tubes, because of the better tube wetting.

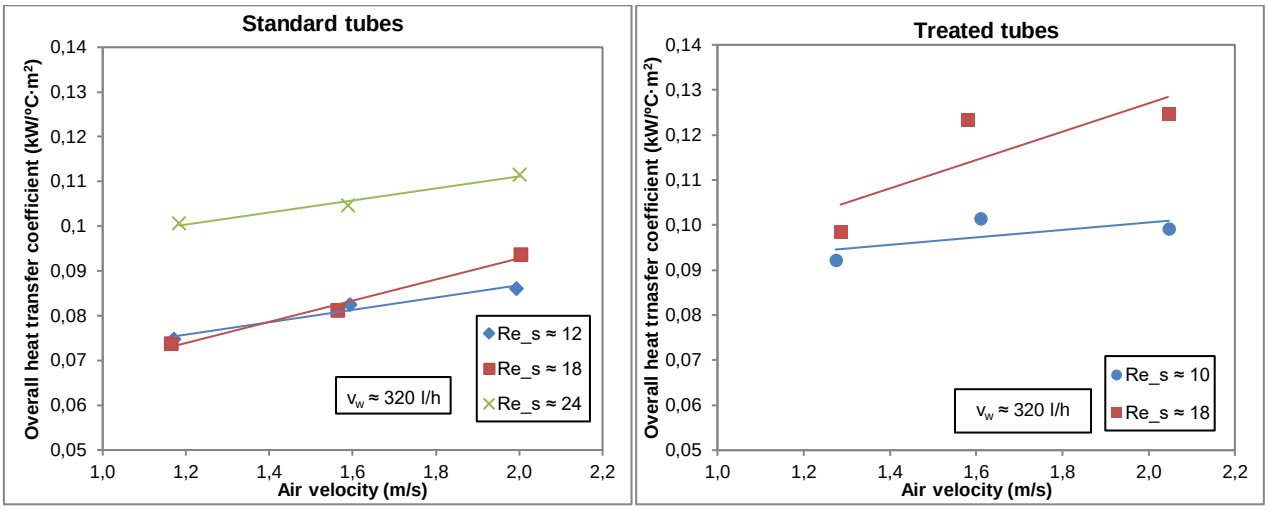

Figure 5. Overall heat transfer coefficient of the absorbers as a function of the air velocity and the Reynolds number of the solution

Absorber heat duty (Figure 6) mainly depends on the air velocity and the difference between the inlet temperatures of the solution and the cooling water streams. Again, the higher the air velocity, the higher the absorber heat duty is because of the increase in the overall heat transfer coefficient. Similarly, the higher the temperature difference between the water and solution, the higher the absorber heat duty is.

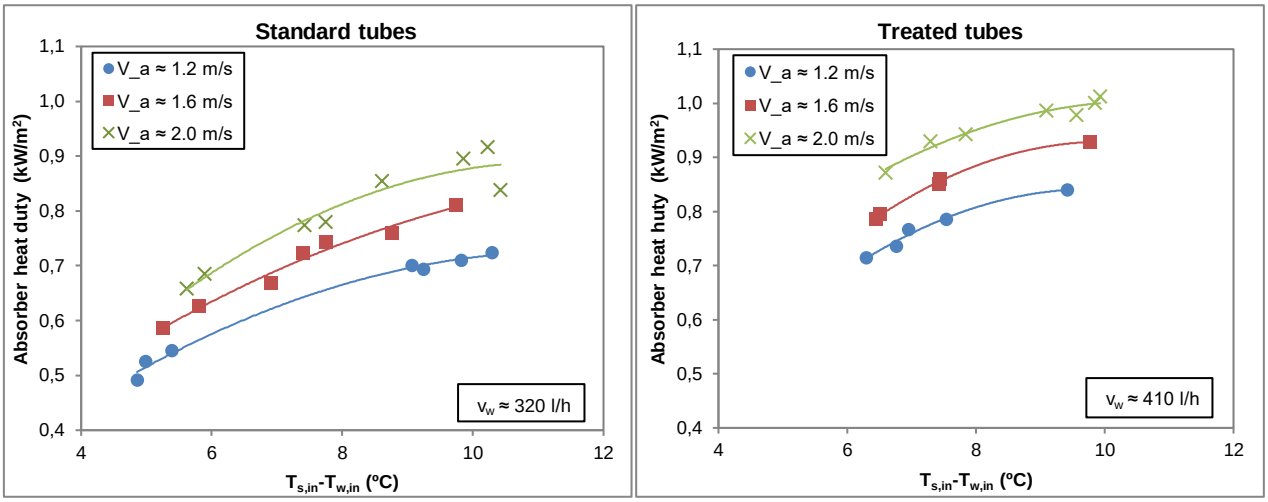

Figure 6. Absorber heat duty as a function of the temperature difference between the inlet solution and inlet water and air velocity

The air cooling rate of the absorber (Figure 7 and Figure 8) depends on the air velocity, the inlet liquid desiccant temperature and, to some extent, the Reynolds number of the liquid desiccant in the absorber with treated polypropylene tubes. Like the previous parameters, the higher the air velocity, the higher the air

cooling rate in the absorbers. In this case, this effect is not due only to a better heat transfer but also to a better air-liquid desiccant mass transfer.

However, the Reynolds number of the solution flow does not seem to cause a big change in the air cooling rate in the absorber with standard tubes. This effect is because the tube wetting of the tubes is not enhanced much by increasing solution flow rates. In both absorbers, the inlet liquid desiccant temperature has a considerable effect on the air cooling rate. In this respect, the lower the inlet liquid desiccant temperature the higher the air cooling rate. This is because dehumidification is improved by the lower vapor pressure of water in the liquid desiccant and higher sensible cooling in air.

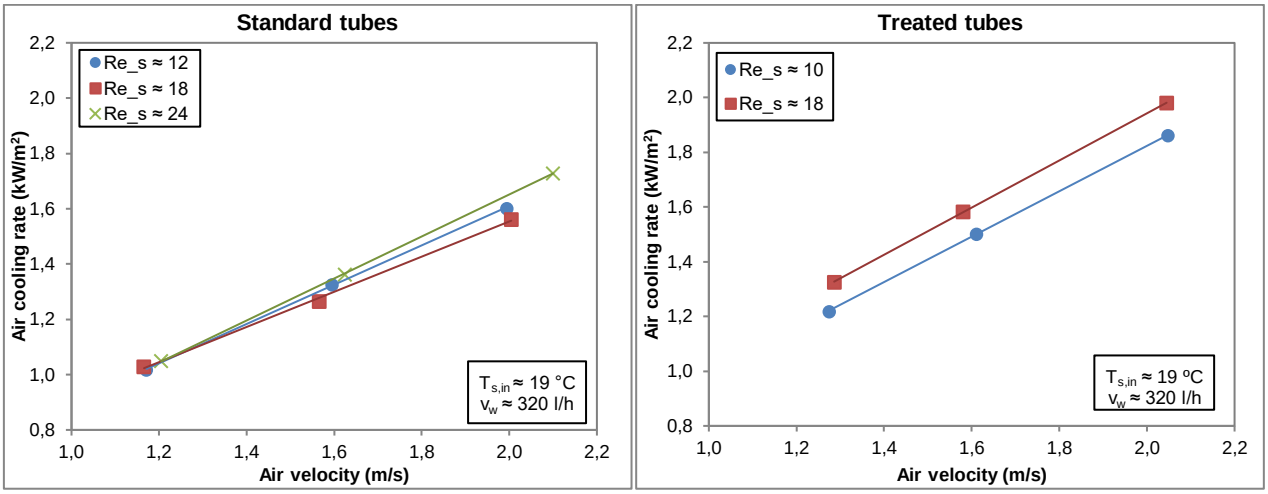

Figure 7. Air cooling rate of the absorbers as a function of the air velocity and the Reynolds number of the solution

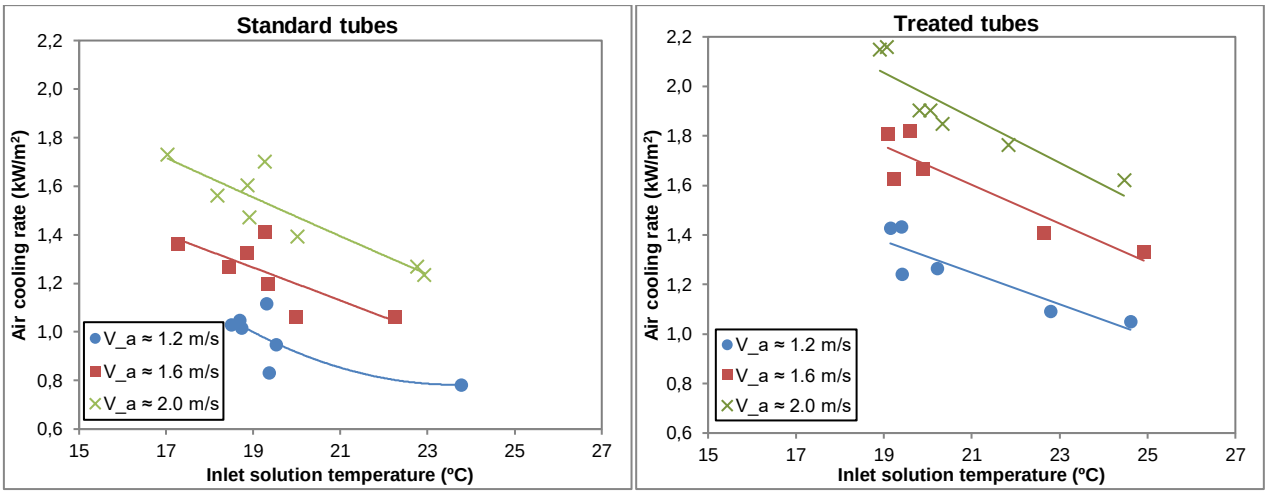

Figure 8. Air cooling rate of the absorbers as a function of the air velocity and the inlet solution temperature

The inlet solution temperature and the air velocity are the variables that have the highest influence on the air dehumidification rate (Figure 9). The reasons for this effect are the same as those for the air cooling rate. However, the solution flow Reynolds number which, in principle, could affect the dehumidification, has a negligible influence on it compared to the other two variables. Therefore, these two variables can be used to control the supply humidity ratio in a liquid desiccant system.

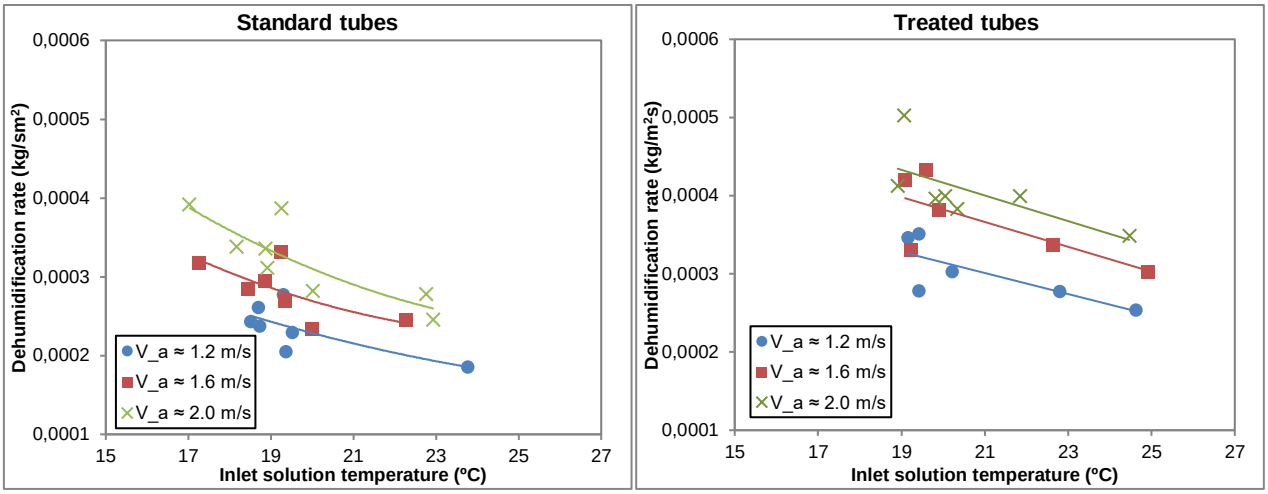

Figure 9. Air dehumidification rate of the absorbers as a function of the inlet solution temperature and the air velocity

3.2. Comparison of absorber performance

Figure 10 and Figure 11 compare the two absorbers in terms of heat duty, overall heat transfer coefficient, air cooling rate and dehumidification rate under similar working conditions. In this regard, the absorber with treated tubes performs better than the absorber with standard tubes in all these four variables. More specifically, the heat duty in the absorber with treated tubes is enhanced by about 70 W throughout the range of air velocities, which means an improvement of about 17 % over the standard tubes. With treated tubes, the overall heat transfer coefficient increases slightly at higher air velocities; the maximum difference is 0.026 kW/ºC (which is obtained at 2 m/s), which is an improvement of 54 % in comparison with the absorber with standard polypropylene tubes.

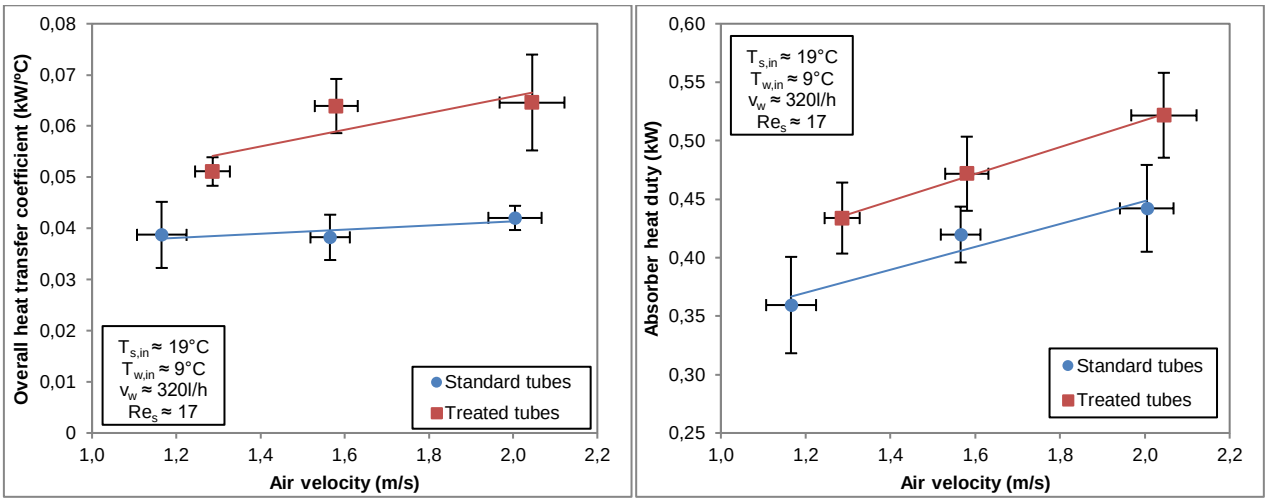

Figure 10. Comparison of the absorbers' overall heat transfer coefficient (left) and heat duty (right) as a function of the air velocity

Similarly, the enhancement of the air cooling rate achieved with treated tubes increases slightly at higher air velocities; the maximum difference is 232 W, which is about 29 % in comparison with the standard tubes. Finally, the maximum improvement in the dehumidification rate achieved by the treated tubes is $6.9 \cdot 10^{-5}$ kg/m^{2}s, which is an enhancement of about 20 % in comparison with standard tubes.

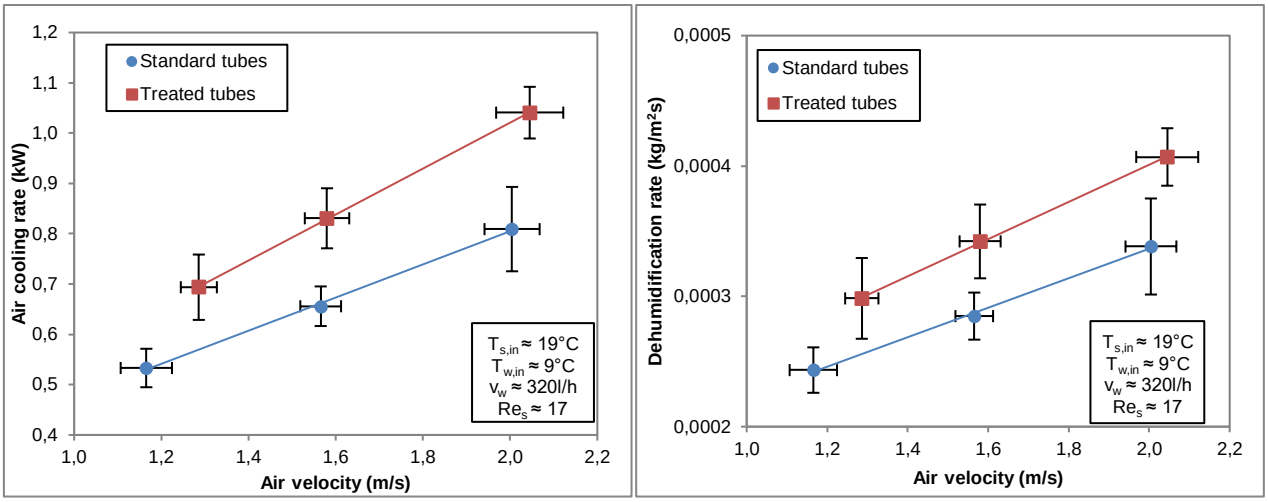

Figure 11. Comparison of the air cooling rate and (left) the dehumidification rate (right) as a function of air velocity

4. Conclusions

Experimental tests were carried out at absorber working conditions to determine the performance of two polypropylene falling-film air-solution contactors with horizontal tubes of a liquid desiccant system. The absorbers were of the same dimensions and specifications with the exception of the tube surface. The heat duty, air cooling rate, overall heat transfer coefficient and dehumidification rate were the variables used to study and compare their performance. The main difference between them is that one was subject to a plasma surface treatment to improve its wettability.

According to the data analysis of the present study, air velocity and inlet liquid desiccant temperature are the variables that have the highest effect on the absorber performance. In particular, air cooling and dehumidification rate are increased about 50 % and 37 % respectively when air velocity is increased from 1.2 to 2.0 m/s. Similarly, air cooling and dehumidification rate are risen about 35 % and 52 % respectively when inlet solution temperature is decreased from 23 to 17 °C. The effect of the air velocity is due to an improvement in the mass transfer and in the tube-solution heat transfer coefficient. The inlet liquid desiccant temperature mostly affects the dehumidification rate and the air cooling rate. In this case, lower inlet liquid desiccant temperatures reduce the vapour pressure of the water within the desiccant, so the dehumidification rate increases. As well as this effect, the air cooling rate increases because of the sensible cooling of air is greater. Thus, these two variables can be used to control the air dehumidification and air cooling rate in a liquid desiccant system.

The liquid desiccant flow rate, which in principle can play a key role in the absorber performance, only affects the overall heat transfer coefficient, which is enhanced when the solution Reynolds number is higher than 10 for the treated tubes and when the solution flow Reynolds number is higher than 18 for the standard tubes.

Our comparison of the two absorbers showed that the absorber with treated tubes performed better. The enhancement is the greatest for the overall heat transfer coefficient (up to 54 %), but also considerable for the absorber heat duty (about 17 %), air cooling rate (up to 29 %) and dehumidification rate (20 %), which shows that tube wetting is much better in the treated polypropylene tubes.

5. Acknowledgement

This work has been supported by the European Nanocool project (ref n. 314701) co-founded by the EC under FP7-2012-NMP-ENV-ENERGY-ICT-EeB.

References

[1] L. Mei, Y.J. Dai, A technical review on use of liquid-desiccant dehumidification for air-conditioning application, Renew. Sustain. Energy Rev. 12 (2008) 662–689. doi:10.1016/j.rser.2006.10.006.

[2] A.Y. Khan, F.J. Sulsona, Modelling and parametric analysis of heat and mass transfer performance of refrigerant cooled liquid desiccant absorbers, Int. J. Energy Res. 22 (1998) 813–832.

[3] K. Gommed, G. Grossman, Experimental investigation of a liquid desiccant system for solar cooling and dehumidification, Sol. Energy. 81 (2007) 131–138. doi:10.1016/j.solener.2006.05.006.

[4] S. Yamaguchi, J. Jeong, K. Saito, H. Miyauchi, M. Harada, Hybrid liquid desiccant air-conditioning system: Experiments and simulations, Appl. Therm. Eng. 31 (2011) 3741–3747. doi:10.1016/j.applthermaleng.2011.04.009.

[5] A. Coca-Ortegón, J. Prieto, A. Coronas, Modelling and dynamic simulation of a hybrid liquid desiccant system regenerated with solar energy, Appl. Therm. Eng. 97 (2016) 109–117. doi:10.1016/j.applthermaleng.2015.10.149.

[6] J. Prieto, J. Ortiga, X. Peña, L. Alonso, K. Gommed, G. Grossman, A. Coronas, Experimental analysis of a hybrid liquid desiccant system with non-adiabatic air-solution contactors at different working conditions, in: P.K. Heiselberg (Ed.), CLIMA 2016 - Proc. 12th REHVA World Congr. Vol. 9, Aalborg, Denmark, n.d.

[7] J. Prieto, Theoretical and experimental study of a dehumidification system based on liquid desiccants for air conditioning applications, Disertation, Universitat Rovira i Virgili, 2016. http://hdl.handle.net/10803/387317.

[8] K. Systems, Kathabar Systems http://www.kathabar.com/index.php/liquid-desiccant/liquid-literature, 2012 (2015).

[9] C. Dyna Air ltd, Dyna-air dryer system, Http://www.dyna-Air.jp/. (2016).

[10] A. Systems, Advantix Systems http://www.advantixsystems.com/downloads.php, 2012 (2014).

[11] K. Gommed, G. Grossman, F. Ziegler, Experimental Investigation of a LiCl-Water Open Absorption System for Cooling and Dehumidification, J. Sol. Energy Eng. 126 (2004) 710–715. doi:10.1115/1.1643075.

[12] P. Bansal, S. Jain, C. Moon, Performance comparison of an adiabatic and an internally cooled structured packed-bed dehumidifier, Appl. Therm. Eng. 31 (2011) 14–19. doi:10.1016/j.applthermaleng.2010.06.026.

[13] M. Badami, J.C. Bruno, A. Coronas, J. Ortiga, A. Portoraro, Preliminary Experimental Results of a Liquid Desiccant Cooling System and Comparison With Empirical Correlations, in: 9th IIR Gustav Lorentzen Conf., 2010.

[14] E. Lävemann, M. Peltzer, Distributor for Micro-quantities of liquid, US 7021608, 2006.

[15] W. Kessling, E. Lävemann, C. Kapfhammer, Energy storage for desiccant cooling systems component development, Sol. Energy. 64 (1998) 209–221.

[16] A. Lowenstein, M. Sibilia, J. Miller, T.S. Tonon, Heat exchanger assembly, 2004.

[17] Y. Yonggao, Z. Xiaosong, W. Geng, L. Lei, Experimental study on a new internally cooled/heated dehumidifier/regenerator of liquid desiccant systems, Int. J. Refrig. 31 (2008) 857–866. doi:10.1016/j.ijrefrig.2007.10.004.

[18] J. Liu, T. Zhang, X. Liu, J. Jiang, Experimental analysis of an internally-cooled/heated liquid desiccant dehumidifier/regenerator made of thermally conductive plastic, Energy Build. 99 (2015) 75–86. doi:10.1016/j.enbuild.2015.04.023.

[19] A. Lowenstein, Review of Liquid Desiccant technology for HVAC Applications, HVAC&R Res. 14 (2008) 819–839.

[20] K. Gommed, G. Grossman, J. Prieto, J. Ortiga, A. Coronas, Experimental comparison between internally and externally cooled air-solution contactors, Sci. Technol. Built Environ. 21 (2015) 267–

274. doi:10.1080/23744731.2015.1015381.
[21] A. Fina, A. Guerriero, S. Colonna, F. Carosio, G. Saracco, Polymer-based materials for the application in Liquid Dessicant heat exchangers, in: V Congr. Iberoam. Ciencias Y Técnicas Del Frío, Tarragona, Spain, 2014.
[22] R.W. Hyland, A. Wexler, Formulations for the Thermodynamic Properties of the Saturated Phases of H20 from 173.15 K to 473.15 K, 1983.
[23] L. Haar, J.S. Gallagher, G.S. Kell, Thermodynamic and Trnasport Properties and Computer Programs for Vapor and Liquid of Water in S.I. Units., Hemisphere, Washington, D.C., 1984.
[24] J. Pátek, J. Klomfar, Thermodynamic properties of the LiCl-H2O system at vapor-liquid equilibrium from 273 K to 400 K, Int. J. Refrig. 31 (2008) 287–303. doi:10.1016/j.ijrefrig.2007.05.003.
[25] M.R. Conde, Properties of aqueous solutions of lithium and calcium chlorides: formulations for use in air conditioning equipment design, Int. J. Therm. Sci. 43 (2004) 367–382. doi:10.1016/j.ijthermalsci.2003.09.003.
[26] W.M. Bowman, R.A.; Mueller, A.C.; Nagle, Mean Temperature Diference in Design, Trans. ASME. 62 (1940) 283.
[27] S.J. Kline, F.A. McClintock, Describing uncertainties in single-sample experiments, Mech. Eng. 75 (1953) 3–8.
[28] R. Armbruster, J. Mitrovic, Heat transfer in falling film flow on a horizontal tube, in: Proc. 30th Natl. Heat Transf. Conf. ASME, Portland, USA, 1995: pp. 13–21.

Appendix

Table A.1. Experimental results of the absorber with standard polypropylene tubes

No.	$T_{s,in}$ (ºC)	$T_{s,out}$ (ºC)	$H_{a,in}$ (%)	V_a (m/s)	$T_{a,in}$ (ºC)	$H_{a,out}$ (%)	$T_{a,out}$ (ºC)	$v_{s,in}$ (l/h)	$T_{w,in}$ (ºC)	$T_{w,out}$ (ºC)	v_w (l/h)	$X_{s,in}$ (%)
1	17.7	20.4	48.5	1.78	27.0	42.9	21.8	222.9	13.3	14.3	220.4	35.9
2	19.9	22.8	39.4	2.06	28.2	39.2	22.0	221.7	8.8	10.3	276.3	35.7
3	17.0	19.4	35.5	2.10	32. 6	37.9	24.2	313.7	10.2	11.2	321.5	35.9
4	17.3	19.2	42.2	1.62	29.5	40.8	22.6	310.8	9.5	10.6	318.8	35.9
5	18.7	19.9	46.3	1.20	28.2	41.5	21.7	314.7	8.9	9.9	311.7	35.9
6	18.2	20.8	43.1	2.00	29.2	40.4	24.0	215.1	9.6	10.7	323.9	35.8
7	18.4	20.3	41.1	1.57	29.9	41.2	22.9	212.9	8.7	9.8	321.9	35.9
8	18.5	20.1	44.7	1.17	28.8	42.6	21.7	212.0	9.3	10.2	321.1	35.8
9	18.7	20.4	44.3	1.17	29.1	43.1	22.0	159.4	9.7	10.6	323.4	35.9
10	18.8	20.9	42.0	1.59	29.8	42.8	22.6	158.5	10.1	11.1	322.4	35.8
11	18.9	21.3	38.4	1.99	30.9	41.0	23.3	158.1	8.7	9.9	320.9	35.9
12	18.9	21.5	39.1	2.01	30.8	41.7	24.0	156.2	13.0	14.0	325.2	35.7
13	19.3	21.6	41.2	1.56	30.4	42.0	23.7	155.3	13.5	14.4	322.1	35.6
14	19.5	20.8	44.7	1.15	29.6	42.9	23.2	154.8	14.1	14.9	319.6	35.8
15	19.4	20.5	44.6	0.99	29.2	41.3	22.8	220.6	14.5	15.2	322.1	35.9
16	19.3	21.2	39.4	2.00	31.6	39.9	24.3	299.7	13.7	14.6	316.0	35.7
17	19.3	21.2	41.0	1.59	31.1	40.3	23.9	298.0	14.0	14.9	309.8	35.8
18	19.3	20.8	43.7	1.18	30.4	40.1	23.4	297.0	14.3	15.1	310.7	35.8
19	20.0	22.1	35.8	2.07	29.2	37.0	22.7	230.5	10.2	11.4	321.5	35.7
20	22.9	24.4	36.7	2.06	29.4	38.9	23.5	134.2	12.5	13.7	322.0	35.7
21	20.0	22.1	39.2	1.63	28.9	39.1	23.1	133.7	13.1	14.0	322.8	35.7
22	23.8	25.0	41.7	1.21	28.4	39.6	23.2	133.3	13.5	14.5	316.4	35.7
23	22.3	23.3	39.5	1.60	29.3	38.1	23.8	303.8	14.9	15.9	325.7	35.8
24	22.8	24.1	37.2	2.08	30.1	37.4	24.6	300.8	15.3	16.4	325.4	35.7

Table A.2. Experimental results of the absorber with treated polypropylene tubes

No.	$T_{s,in}$ (°C)	$T_{s,out}$ (°C)	$H_{a,in}$ (%)	V_a (m/s)	$T_{a,in}$ (°C)	$H_{a,out}$ (%)	$T_{a,out}$ (°C)	$v_{s,in}$ (l/h)	$T_{w,in}$ (°C)	$T_{w,out}$ (°C)	v_w (l/h)	$X_{s,in}$ (%)
1	17.9	18.7	42.6	1.27	29.5	41.7	21.2	123.3	9.6	10.6	322.2	35.6
2	18.3	19.5	39.7	1.61	30.1	42.1	21.2	122.5	10.1	11.2	321.9	35.7
3	18.5	19.9	37.0	2.05	30.9	41.3	21.6	122.6	8.8	10.1	321.7	35.6
4	18.0	18.3	36.5	2.04	31.2	39.6	21.5	233.9	9.4	10.8	322.4	35.7
5	17.9	18.1	38.6	1.58	30.7	39.9	21.3	233.2	9.9	11.2	322.5	35.7
6	17.9	17.8	40.4	1.29	30.2	39.7	21.1	232.1	8.7	9.9	322.9	35.6
7	19.1	21.0	44.6	2.08	31.5	46.0	22.8	343.8	11.2	12.3	411.6	35.7
8	19.1	20.7	43.7	1.62	32.1	45.1	22.6	342.0	11.7	12.6	412.3	35.7
9	19.2	20.4	45.4	1,19	31.8	44.2	22.3	340.3	12.2	13.0	411,6	35.7
10	19,4	20.8	46.6	1,20	31.5	44.9	22.2	259.1	12.6	13.4	410.3	35.7
11	19.6	21.3	44.7	1.64	31.9	45.2	22.8	255.1	13.1	13.9	412.5	35.7
12	19.9	21.8	43.8	1.63	32.1	46.6	23.3	171.3	13.4	14.3	412.0	35.7
13	20.2	21.7	45.9	1.21	31.6	46.6	23.1	170.9	13.9	14.7	413.5	35.7
14	25.0	26.1	36.1	2.09	31.9	39.5	24.4	172.2	15.9	16.8	423.5	35.4
15	24.6	25.2	40.6	1.21	31.4	38.5	24.5	257.1	17.1	17.9	417.5	35.5
16	24.9	25.7	37.9	1.63	32.3	38.2	25.2	256.4	17.5	18.4	421.8	35.6
17	24.5	25.7	35.2	2.08	33.2	37.1	25.9	255.8	17.9	18.8	423.0	35.6
18	18.9	20.8	33.2	2.07	33.6	39.1	22.7	345.4	9.0	10.1	409.8	35.3
19	19.2	20.8	35.7	1.53	32.8	40.0	22.2	343.3	9.5	10.5	405.4	35.5
20	19.4	20.5	40.1	1.12	31.5	40.3	21.7	341.5	10.0	10.9	406.7	35.5
21	19.8	21.5	38.3	1.99	31.8	42.1	22.5	343.7	10.7	11.8	410.8	35.5
22	20.1	21.2	38.6	1.99	31.7	42.0	22.5	232.4	10.2	11.3	408.9	35.4
23	20.3	21.7	38.9	2.00	31.7	43.2	22.7	160.6	10.8	11.8	411.0	35.5
24	21.8	24.0	41.4	2.09	31.2	42.6	23.8	330.9	14.6	15.5	423.2	35.4
25	22.6	25.0	43.0	1.64	30.9	42.0	23.4	329.6	14.9	15.9	423.5	35.4
26	22.8	25.4	45.7	1.21	30.4	42.0	23.8	328.4	15.3	16.2	423.5	35.3